CHEMISTRY
A EUROPEAN JOURNAL

DOI: 10.1002/chem.200601706

Elucidating the Mechanism of the Asymmetric Aza-Michael Reaction

Pim Huat Phua,[a] Suju P. Mathew,[a] Andrew J. P. White,[a] Johannes G. de Vries,[b] Donna G. Blackmond,[a] and King Kuok (Mimi) Hii*[a]

Abstract: The mechanism of the palladium-catalysed asymmetric aza-Michael addition of aniline to α,β-unsaturated *N*-imide was examined from several aspects using a combination of techniques, including X-ray crystallography, mass spectrometry, NMR, UV/Vis spectroscopy, and kinetic studies. The binding of aniline to the dicationic palladium(II) metal centre was found to occur in two consecutive steps: The binding of the first aniline is fast and reversible, whereas the binding of the second aniline is slower and irreversible. This occurs in competition with the binding of the N-imide, which forms a planar six-membered chelate ring with the metal centre; coordinating through the 1,3-dicarbonyl moiety. Isotopic labelling revealed that the addition of N-H occurs in a highly stereoselective manner, allowing the synthesis of optically active β^2- and $\beta^{2,3}$-amino acid derivatives. The stereochemistry of the addition is postulated to be *syn*. In situ kinetic studies provided evidence for product inhibition. The binding of the *N*-imide to the catalyst was found to be the rate-limiting step. Aniline was found to be an inhibitor of the pre-catalyst. The study culminated in the design of a new reaction protocol. By maintaining a low concentration of the aniline substrate during the course of the reaction, significant enhancement of yield and enantioselectivity can be achieved.

Keywords: asymmetric catalysis · kinetics · Michael addition · palladium · reaction mechanism

Introduction

In previous work, we demonstrated that the air- and moisture-stable dicationic palladium complex [((*R*)-BINAP)Pd-$(OH_2)_2]^{2+}[TfO]^-_2$ (**1**; see below) can effect highly enantioselective addition of aromatic amines to a number of Michael acceptors (**2**–**4**) that contain chelating dicarbonyl moieties (Scheme 1).[1]

We believed that the cationic palladium catalyst acts as a chiral Lewis acid in these reactions, activating the unsaturated double bond towards nucleophilic attack, through the chelation of the 1,3-dicarbonyl functionality. Subsequent catalyst screening revealed that other dicationic palladium complexes are also catalytically active in these reactions. However, only ones that contain diphosphine ligands furnish good turnovers, and those containing a C_2-symmetrical chiral biaryl unit, typified by the BINAP complex **1**, afford the highest enantioselectivities.[2] In terms of substrate scope, the choice of the chelating imide functionality (*N*-oxazolinone, *N*-benzoyl or *N*-carbamate) has been shown to exert a significant effect on the catalytic turnover and selectivity.[1c] For example, the addition to *N*-oxazolinones **2** required typically 10 mol% of **1**, while the addition to *N*-carbamates **3** can proceed with quantitative conversion and perfect enantioselectivity, using just 2 mol% of the catalyst.

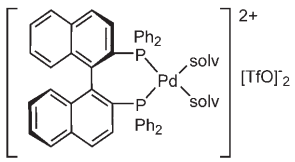

(*R*)-**1**
(solv = CH_3CN, H_2O)

In all cases, the reaction outcome is dependent on the electronic nature of the aromatic amine. The employment of electron-rich amines generally has a detrimental effect on

[a] P. H. Phua, Dr. S. P. Mathew, Dr. A. J. P. White, Prof. D. G. Blackmond, Prof. K. K. Hii
Department of Chemistry, Imperial College London
Exhibition Road, South Kensington, London SW72AZ (UK)
Fax: (+44) 20-7594-1142
E-mail: mimi.hii@imperial.ac.uk

[b] Prof. J. G. de Vries
DSM Pharmaceutical Products
Advanced Synthesis Catalyst & Development
P.O. Box 18, 6160 MD Geleen (The Netherlands)

Supporting information for this article is available on the WWW under http://www.chemeurj.org/ or from the author.

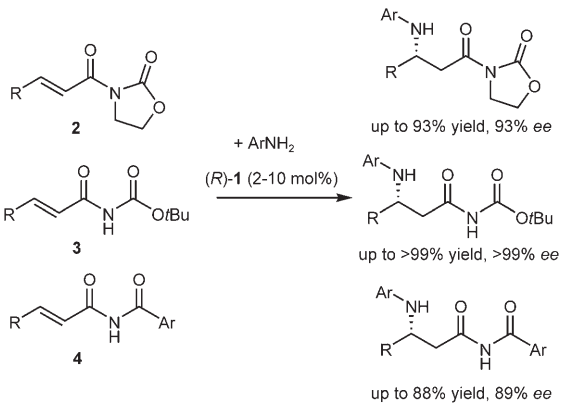

Scheme 1. Enantioselective aza-Michael addition catalysed by complex (*R*)-**1**.

yield and selectivity. Proposing that nucleophilic amines deactivate the dicationic palladium catalyst, Sodeoka et al. employed ammonium triflate salts as reactive substrates for the addition to *N*-oxazolidinones **2**.[3] Using the dimeric μ-hydroxy complex **5** as a catalyst, controlled release of the amine can be achieved, and impressive results were obtained for the addition of aromatic and benzylamines (Scheme 2). However, the reaction requires a stoichiometric

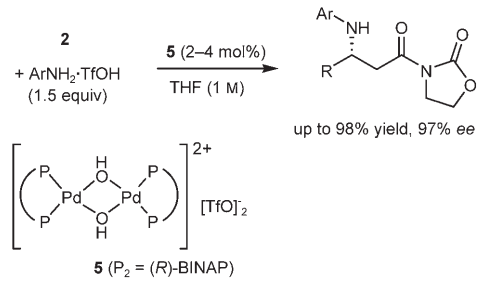

Scheme 2. Amine salt-controlled addition of amine-triflate salts.

amount of triflic acid in the preparation of the amine salt. In order to preserve the perfect atom economy of the process, we favoured an approach whereby the problem can be overcome by adjusting the reaction protocol. To this end, we initiated a study to delineate key steps of the reaction, so as to gain a clearer understanding of the catalyst deactivation process, especially in relation to the catalytic turnover.

Results and Discussion

The addition of aniline to butenoyl-*N*-imide **4a** catalysed by complex (*R*)-**1** was chosen as the model for the present study (Scheme 3). All the investigations were carried out with THF as the solvent to maintain homogeneity, and to ensure compatibility of results between different experiments.[4]

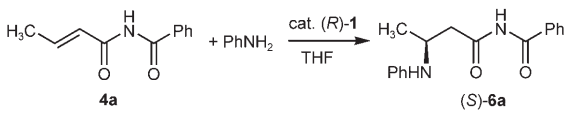

Scheme 3. Aza-Michael reaction between aniline and *N*-butenoyl imide **4a**.

Amine coordination: Previously, we showed that the μ-hydroxy palladium complex **5** is much less active than the monomeric complex **1** in catalysing these additions.[2] Work by other groups have shown that the coordination of H_2O or $ArNH_2$ to dicationic (diphosphine)palladium(II) complexes renders the O–H and N–H bonds acidic, which can be deprotonated to give μ-hydroxy or anilide complexes, respectively.[5,6] With this in mind, the coordination of aniline to **1** was examined, to establish whether any such dimeric species are involved in the catalytic process.

The addition of two equivalents of aniline to complex **1** in [D_8]THF ($\delta P = +32$ ppm) generated a complex mixture of broad and sharp ^{31}P resonance signals between 21.2–29.8 ppm. Increasing the temperature to 60 °C caused these signals to coalesce at 26.4 ppm. This suggests that the binding of the aniline to **1** is a highly fluxional process involving several exchanging species, which could be the result of restricted rotation of the coordinated aniline, and competitive binding of the solvent (THF, water) or the triflate anion to the cationic metal centre.[7,8]

The formation of a diamine complex, nominally formulated as $[((R)\text{-BINAP})Pd(NH_2Ph)_2]^{2+}[TfO]^-_2$ (**7**), can be detected by ESI mass spectrometry, which revealed a doubly charged ion at m/z 1145. Its isotopic distribution pattern is an excellent match to that calculated for a solvated diamine palladium complex ion $[\{(BINAP)Pd(NH_2Ph)_2(OTf) + 2\,CH_3CN\}_2]^{2+}$ (Figure 1).

Utilising the faster timescale afforded by UV/Vis spectroscopy, the coordination of amine was examined by monitoring changes in the chromophore of complex **1** in the presence of varying amounts of aniline.[9] A solution of **1** in THF displayed three absorption bands at $\delta = 311$, 328 and 376 nm. Successive introduction of small quantities (0.02 equiv) of aniline caused the gradual disappearance of the absorption peak at 376 nm and an increased intensity at 328 nm. By adding up to one equivalent of the aniline, a distinctive isosbestic point was observed at 365 nm (Figure 2), indicating the formation of a chemically distinct complex, tentatively attributed to the mono-amine complex $[(BINAP)Pd(NH_2Ph)(OH_2)]^{2+}[TfO]^-_2$ (**8**). The binding of a single aniline molecule is a reversible process, as the addition of water cause the equilibrium to be re-established instantaneously towards the starting complex **1**.

The addition of more than one equivalent of aniline led to the emergence of a new absorption peak at 465 nm, corresponding to the formation of the diamine complex **7** (ESI-MS). In contrast to the binding of the first aniline, the binding of the second aniline to palladium appears to be a slow process (Figure 3). Furthermore, the addition of water did not lead to the dissociation of aniline from this molecule.

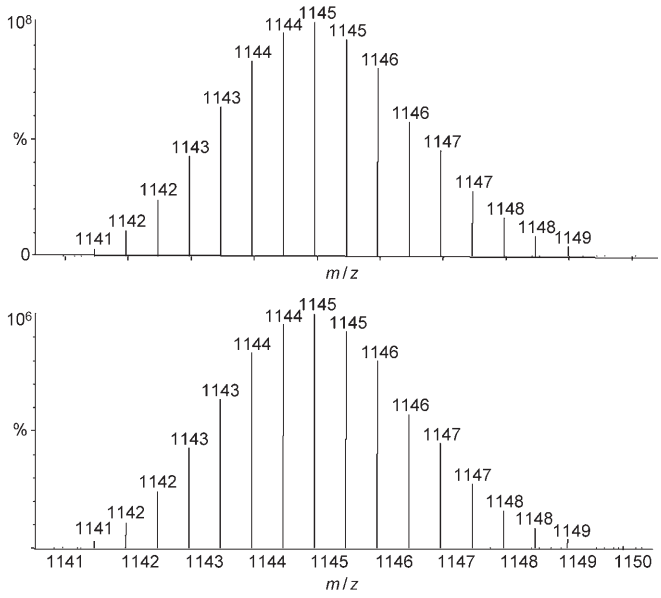

Figure 1. Observed (above) and calculated (below) isotopic distribution patterns for $[\{(BINAP)Pd(aniline)_2(OTf) + 2CH_3CN\}_2]^{2+}$ (m/z 1145); solvent: acetonitrile

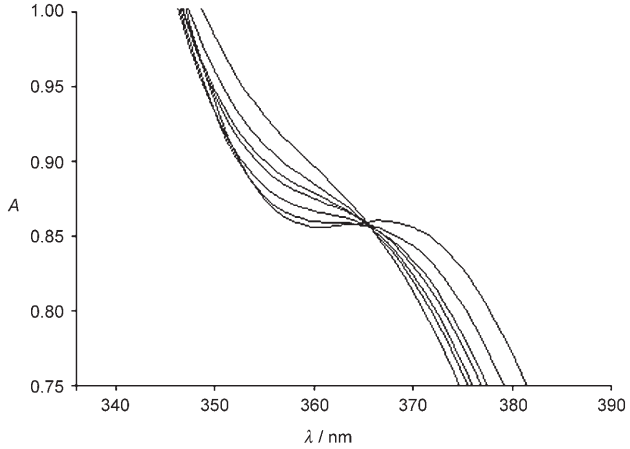

Figure 2. Observed isosbestic point for the binding of one molecule of aniline to complex **1**.

Thus, the UV/Vis experiment revealed that the coordination of aromatic amines to the dicationic palladium complex occurs in two chemically distinct steps (Scheme 4): The coordination of the first aniline is facile and reversible, while the second aniline binds much more slowly. Once established, the diamine complex **7** is kinetically stable and does not dissociate readily.

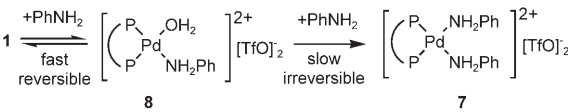

Scheme 4. Consecutive binding of aniline to complex **1**.

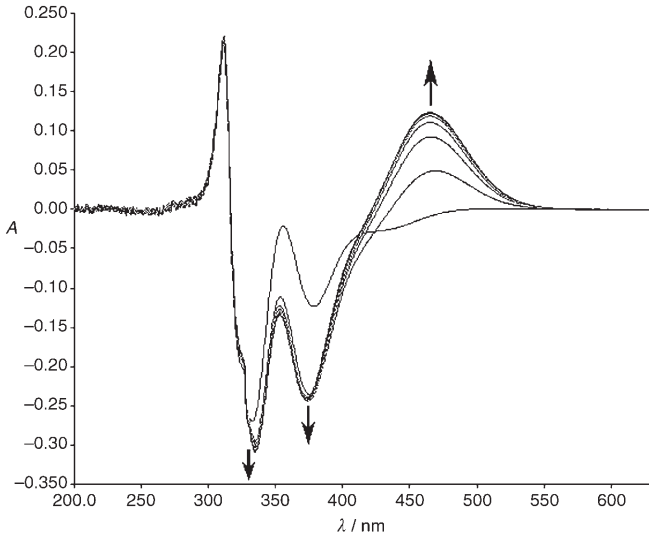

Figure 3. Real-time formation of the diamine complex, recorded by UV/Vis spectroscopy: Aniline (3 equiv) was added to a solution of complex **1** and spectra were recorded consecutively in 15-minute intervals (UV spectrum of complex **1**, $t = 0$, was subtracted from the spectra).

The addition of alkene **4a** to the solution of **7** did not produce significant amounts of **6a**. Hence, the diamine complex is likely to be the catalytically deactivated species. Another notable feature is that the formation of dimeric μ-hydroxy or anilide complexes such as **5**, **9** or **9′** (see below) were

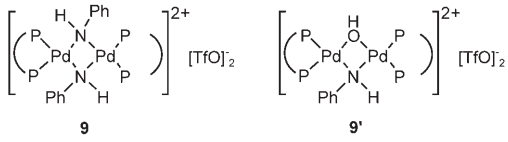

never observed in these experiments, even in the presence of a large excess of aniline at elevated temperature (60 °C).[10] Thus, the involvement of these dimers in the catalytic cycle is highly unlikely.

Alkene coordination: Addition of *N*-imide **4a** to a solution of complex **1** resulted in the slow precipitation of a yellow solid. FAB-MS revealed a mass ion that corresponds to a substrate-bound complex **10** (m/z 917 $[(BINAP)Pd(\mathbf{4a})]^+$). Unfortunately, complex **10** proved to be insufficiently soluble in most organic solvents to enable structure determination by NMR spectroscopy.[11]

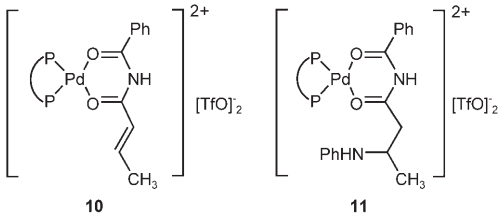

However, by layering solutions of **4a** and **1** carefully, yellow needle-like crystals suitable for X-ray crystallography can be cultivated at the interface. In the solid-state structure (Figure 4), the dicarbonyl moiety of **4a** coordinates to the cationic palladium metal centre to form a planar six-membered chelate ring, the $\{PdC_2NO_2\}$ atoms being coplanar to within about 0.04 Å. The *N*-imide moiety is disordered in the solid-state (Supporting Information), the two orientations being related by an approximate C_2 axis about the Pd···N vector, that is, interchanging the alkenyl and phenyl groups.

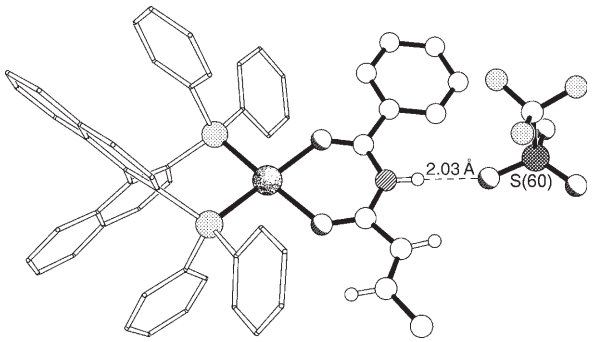

Figure 4. Molecular structures of complex **10**, showing the major (ca. 62%) occupancy orientation of the *N*-imide ligand.

The locations of the two triflate counteranions are especially noteworthy. One of these [based on S(70)], and its symmetry related counterpart [S(70A)], are located within the coordination sphere, the closest approaches to the $\{PdC_2NO_2\}$ plane being about 2.75 and 2.48 Å for the S(70) and S(70A) anions, respectively. However, this anion is disordered and does not show any appreciable interactions with the metal centre—the closest approaches being about 3.03 and 3.02 Å for the S(70) and S(70A) anions, respectively. The S(60) triflate anion, on the other hand, is clearly engaged in hydrogen-bonding to the N-H moiety of the *N*-imide ligand with N···O and H···O separations of 2.911(6) and 2.03 Å, respectively, and an N-H···O angle of 167° (N–H distance normalised to 0.90 Å).

Close examination of the structure did not reveal any significant interactions between the *N*-imide and BINAP moieties that could serve to direct the coordination of the *N*-imide ligand to the palladium–BINAP unit; a pair of possible C-H···π interactions was observed, but these do not seem to distinguish between the phenyl and alkenyl substituents on the *N*-imide ligand (see Supporting Information). This, and the absence of any obvious molecular hindrance that may operate against the approach of a nucleophile from either of the prochiral faces, suggests that the observed enantioselectivity is unlikely to be the result of an early transition state.

Coordination of the product: Interestingly, the product **6a** also displayed substantial affinity to the cationic metal centre. Addition of enantio-enriched **4a** (90% *ee* of the (*S*)-isomer) to complex **1** caused a shift in the ^{31}P resonance signal to $\delta = +30.2$ ppm (broad). As is expected, coordination to the cationic metal caused a broadening and upfield shift of ^1H NMR resonances signals of **4a**, for example, the sharp doublet resonance corresponding to the CH_3 signal moved to $\delta = 1.06$ ppm (from 1.26 ppm). At −50 °C, the ^{31}P resonance resolved into several species, including a singlet at $\delta = +32$ ppm and four AB quartets, identified by $^{31}P,^{31}P$ COSY experiment: a major peak at $\delta P = 25.8$, 29.6 (*J* 20 Hz) and three others at $\delta P = 24.8$, 30.0 (*J* 24 Hz); $\delta P = 26.7$, 29.2 (*J* 20 Hz); and $\delta P = 31.1$, 33.9 (*J* 36 Hz). From this, we surmise that product binding is highly labile, and it can adopt several coordination modes, including combinations of *N*- and *O*-binding through amino and carbonyl groups.

The involvement of palladium complexes **10** (see below) in the catalytic cycle was verified by the addition of a stoichiometric amount of aniline, which led to the formation of **6a** instantaneously. A further experiment was performed, whereby the reaction was monitored by NMR spectroscopy during catalytic turnover (0.2 mmol **4a**, 2 equiv aniline, 1 mL $[D_8]$THF, 5 mol% **1**). At the onset of the reaction, a broad ^{31}P resonance corresponding to complex **1** was detected as the major species in solution. As the reaction progressed (indicated by the emergence of ^1H NMR signal corresponding to **6a**), the signal sharpened and persisted, until a broad peak corresponding to the diamine–palladium complex **7** eventually emerged (26 ppm) towards the end of the reaction. This experiment revealed two important aspects of this reaction: 1) Complex **1** is involved in the rate-determining step, and 2) the formation of the catalytically deactivated complex **7** is not significantly competitive with catalytic turnover.

Synthesis of *N*-arylated β²- and β²,³-amino acid derivatives: The relative stereochemistry of the N-H addition was established by introducing a deuterium isotope at the α-carbon of the Michael acceptor (2-[D]-**4a**), which reacted with aniline in the presence of complex **1** under optimised reaction conditions (Scheme 5).

^1H NMR analysis of the resultant product 2-[D]-**6a** (86% yield) indicated the exclusive occupation of the deuterium label at one of the diastereotopic positions (Figure 5). Un-

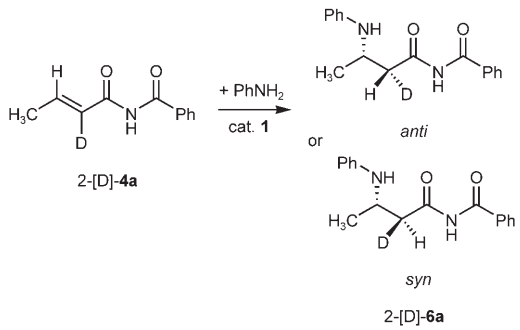

2-[D]-**4a**

2-[D]-**6a**

Scheme 5. Possible stereochemistry of the protonolysis step.

fortunately, subsequent attempts to establish the relative stereochemistry of the methine and methylene protons (by NOE experiments) were thwarted by rapid C(2)–C(3) bond rotation, even at low temperatures. However, as the reaction appears to be a facile process, we tentatively propose the selectivity to be *syn*.

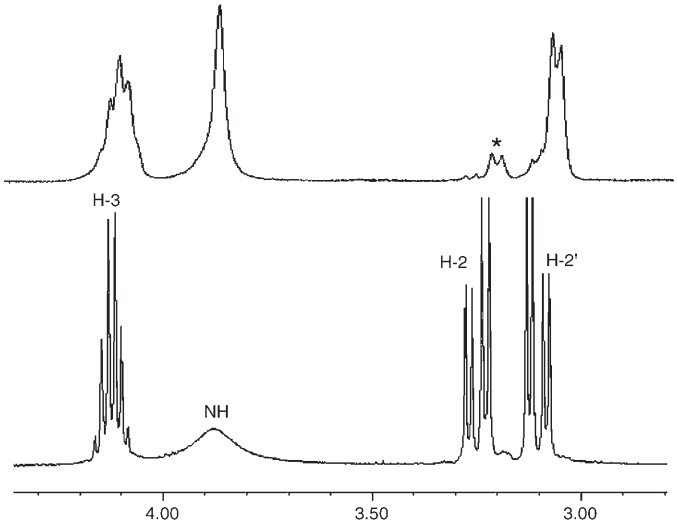

Figure 5. ^{1}H NMR spectra of product obtained from undeuterated (bottom) and deuterated (top) **4a** with aniline. *: Residual proton from incomplete deuteration of precursor.

More significantly, the experiment revealed that the protonolysis at the α-carbon is stereospecific. This implies that the aza-Michael reaction with α-substituted alkene substrates is likely to proceed with good enantioselectivity. Encouraged by this, the addition of aromatic amines to *N*-imide and *N*-carbamate derivatives of methylacrylic and tiglic acids (**12**, **13**, **14** and **15**) were performed in the presence of catalyst **1**, generated in situ from $Pd(OTf)_2$ and (*R*)-BINAP (Scheme 6).[2]

For the addition of aromatic amines (1.5 equivalents) to the *N*-benzoyl methacrylamide derivative **12**, reaction proceeds readily at room temperature. As was observed previously, lower yield and selectivity were obtained from the addition of anisidine, compared with aniline and 4-chloroaniline (Table 1, entries 1–3).[1,2] Thus, while excellent yields of **16a** and **16b** can be obtained in good *ee* values, **16c** can only be obtained in average yield and low *ee*.

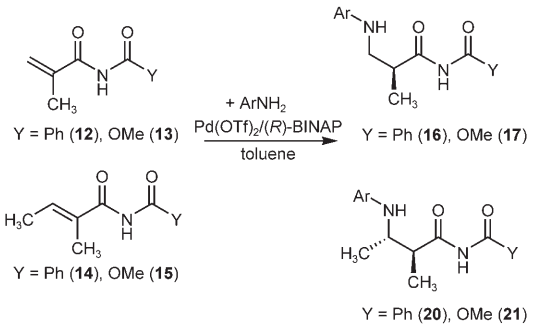

Scheme 6. Synthesis of N-arylated β^2- and $\beta^{2,3}$-amino acids.

Due to limited solubility of the *N*-carbamate derivative **13** in toluene, reactions with this substrate were performed with a lower initial concentration with a slightly elevated temperature at 40 °C.[12] As a result of the higher dilution, the yields were lower compared with the addition to **12**. Nevertheless, yields of between 36–72 % can be obtained with good to high enantioselectivities (up to 85 %) for the addition of less nucleophilic amines to the *N*-carbamate (Table 1, entries 4–6).

Optically active (−)-**16c** may be converted into its parent amino acid, β^2-alanine **19**, by oxidative cleavage of the PMP group with ceric ammonium nitrate, followed by hydrolysis of the *N*-imide group (Scheme 7). The resultant amino acid was found to have the (*S*)-(+)-configuration, by comparison of its optical rotation with the reported value.[13] Hence, the use of (*R*)-**1** leads to the formation of optically enriched products with the (*S*)-configuration. Since the addition to **4a** also proceeded preferentially with (*S*)-stereoselectivity, it added further credence to the hypothesis that the N-H addition occurs at the same face of the alkene.

Table 1. Addition of aromatic amines to **12–15** (Scheme 6).[a]

Entry	Product		*T*/°C	*t*/h	Yield/%[b]	er[c]
1	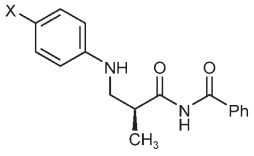	X = Cl (**16a**)	25	18	95	86:14
2		X = H (**16b**)	25	18	95	88.5:11.5
3		X = OMe (**16c**)	25	18	57	69:31
4	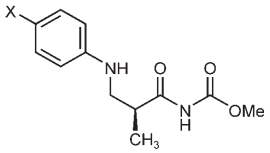	X = Cl (**17a**)	40	18	72	91:19
5		X = H (**17b**)	40	18	59	92.5:7.5
6		X = OMe (**17c**)	40	18	36	77.5:22.5
7[d]	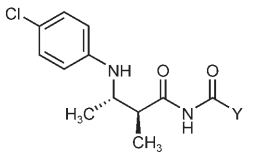	Y = Ph (**20**)	40	48	35	76.5:23.5
8[e]		Y = OMe (**21**)	40	48	25	91.5:8.5

[a] Reaction conditions: 5 mol % $Pd(OTf)_2 \cdot 2H_2O$, 5.5 mol % (*R*)-BINAP, **12** (0.20 mmol), amine (0.22 mmol), toluene (1 mL); or **13** (0.3 mmol), amine (0.2 mmol), toluene (3 mL). [b] ^{1}H NMR integration. [c] Chiral HPLC. [d] **14** (0.20 mmol), 4-chloroaniline (0.30 mmol), toluene (1 mL). [e] **15** (0.20 mmol), 4-chloroaniline (0.22 mmol), toluene (2 mL).

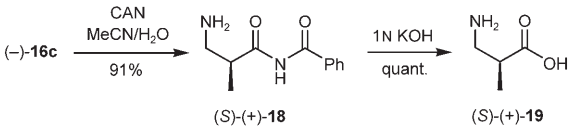

Scheme 7. Conversion of **16c** to β^2-alanine.

Finally, the addition to tigloyl derivatives **14**[14] and **15** was studied. These reactions were extremely sluggish, furnishing low yields even with the most reactive 4-chloroaniline (entries 7 and 8). As expected, the N-H addition occurred stereospecifically. Single diastereomers of **20** and **21**, tentatively assigned with the (*S*,*S*)-configuration, were obtained in 53 and 83% *ee* values, respectively.[15]

Kinetic studies: Reaction progress kinetic analysis was employed to probe the catalytic cycle, allowing us to investigate important factors that influence catalyst stability and the rate of its turnover. In these experiments, data were gathered over the entire course of a reaction under synthetically relevant conditions. With this approach, fewer experiments are required compared with classical kinetic analysis, and results can be easily translated into practice.[16]

Reaction progress was monitored in situ using reaction calorimetry as previously described.[17] A plot of reaction heat flow vs. time is shown in Figure 6 (open circles) for the

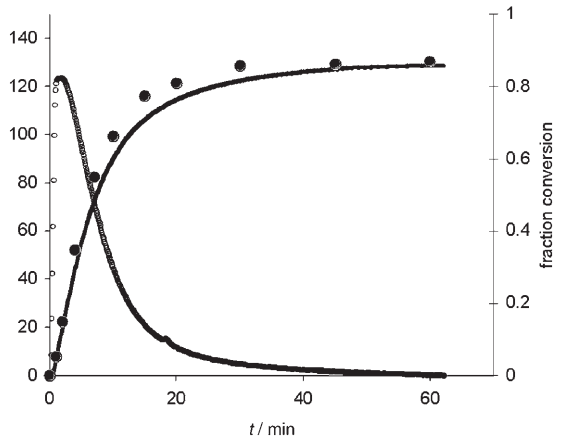

Figure 6. Reaction progress profiled by reaction calorimetry. Reaction conditions: [**4a**] = 0.37 M, [aniline] = 0.56 M, [**1**] = 0.043 M. Reaction heat flow (○, left axis). Conversion vs time (right axis) determined by heat flow (——) and by ^{1}H NMR (●).

addition of aniline to butenoyl *N*-imide **4a** ($\Delta H_{rxn} =$ 45 kJ mol^{-1}). Using 10 mol% of complex **1** in a typical experiment, the reaction occurred spontaneously and was complete within 60 minutes. The heat flow conversion versus time obtained by integration of the reaction heat flow curve (Figure 6, solid line) was compared with conversion versus time obtained by NMR spectroscopy (Figure 6, closed circles). The agreement between the two measurements confirms that the calorimetric measurement furnishes an accurate indication of the progress of the reaction.

Product inhibition ("same excess" experiments): First, the fate of the catalyst over the course of the reaction was examined. Changes in the effective concentration of the catalyst may occur by competitive activation, decomposition or inhibition by the product. Such changes make kinetic analysis problematic unless they may be deconvoluted from the intrinsic kinetics of the steady-state catalytic cycle. A specific protocol, as described previously in reference [16], allows such deconvolution to be followed here: a set of three experiments were performed using different initial concentrations of the two substrates, but holding the "excess" [*e*] constant ([*e*] = the difference between the concentration of **4a** and aniline). Table 2 shows the initial conditions adopted:

Table 2. Initial reaction conditions carried out under conditions of "same excess" [*e*].

component	[**4a**]/M	[$PhNH_2$]/M	[*e*]/M	[**6a**]/M
Expt 1: initial conditions (as above)	0.37	0.56	0.19	0
Expt 2: initial conditions	0.20	0.39	0.19	0
Expt 3: 50% conversion	0.20	0.39	0.19	0.17

Reaction conditions: Catalyst concentration = 0.043 M.

Experiment 3 was designed to mimic the conditions of experiment 1 at 54% conversion, including the amount of product formed. Experiment 2 is identical to experiment 3, except for the absence of added product in the reaction vial.

The results of these three experiments are plotted in Figure 10 in the form of the "graphical rate equation" of reaction rate versus [**4a**]. Because all three experiments have identical reactant concentrations at any given point, the curves in Figure 7 should overlap if the catalyst concentration is at steady-state and is unaffected by influences related to reaction turnover, such as product inhibition. Comparison of curves for experiments 1 and 2 show that the curves are not superimposable (Figure 7), while the plots for experiments 1 and 3 are. This reveals that the driving force represented by the concentrations of reactants is suppressed in the presence of product. Combined with our earlier observation of product-bound complex **11** (see above), this suggests that product inhibition is a significant process during catalytic turnover.

Reaction order in catalyst: Division of the graphical rate equations by the total catalyst concentration [**1**] furnishes TOF versus [**4a**] plots. The normalised TOF plots (Figure 8) show that the reaction is first-order in catalyst, supporting our earlier hypothesis that the involvement of dimeric complexes (e.g. **5** and **9**) is unlikely under catalytic conditions.

The result was further corroborated by performing the reaction described in Scheme 3 with catalyst **1** of different enantiopurity. The enantiomeric excess of the resultant product **6a** was found to vary linearly with the enantiopurity of the catalyst (Figure 9). Thus, we conclude that the catalyst operates through a mononuclear entity during turnover, and that any monomer–dimer equilibria do not distort the active catalyst concentration. Interestingly, a positive non-linear

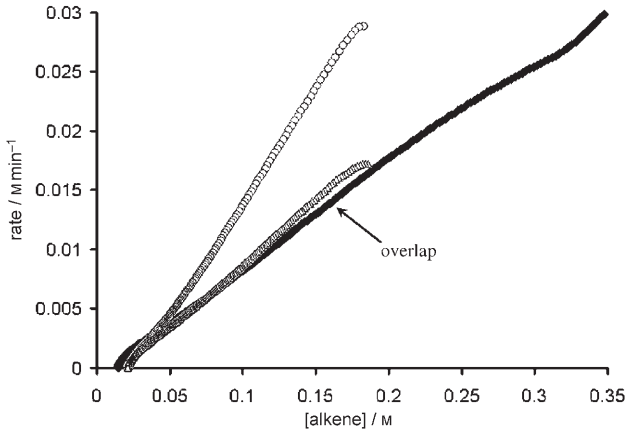

Figure 7. Comparison of rates carried out at the same excess [*e*] under reaction conditions 1 (◆), 2 (○) and 3 (△), as described in Table 1.

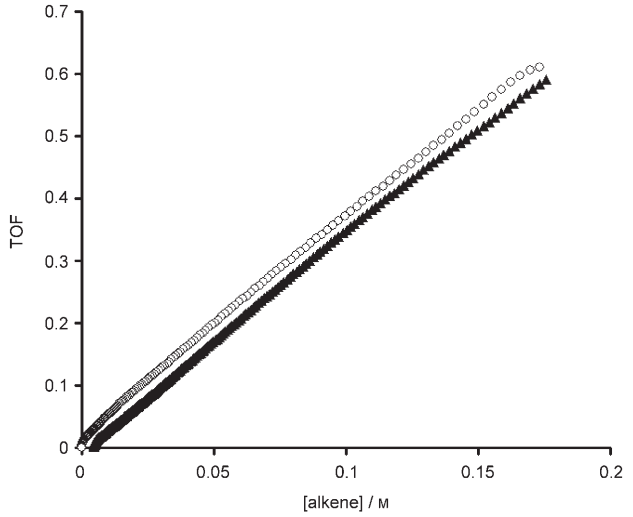

Figure 8. TOF at different catalyst loadings. Reaction conditions were as described for reaction 1 (Table 2), at two different catalyst loadings: ○: 0.061 M, ▲: 0.043 M.

effect was observed when the reaction was carried out in toluene. Concurrently, the *rac*-**1** is found to be significantly less soluble than optically pure (*R*)-**1** in this non-polar medium (i.e., the non-linearity in toluene is attributed to different solubility of diastereomeric conglomerates).[18]

Reaction order in substrates ("different excess" experiments): The kinetic picture surrounding the role of the aniline is more complicated. Spectroscopic study showed that the formation of the diamine complex **7** is detrimental to catalyst activity. Thus, higher concentrations of the amine might be expected to inhibit catalytic activity. Indeed, Figure 10a confirms that higher concentrations of aniline do suppress reaction rate. These data points are extracted from reaction progress curves at the concentrations of alkene **4a** shown. When the same data were plotted as rate divided by [**4a**], data obtained at different [**4a**] fall on the same line, as shown in Figure 10b. This overlay upon normalization by

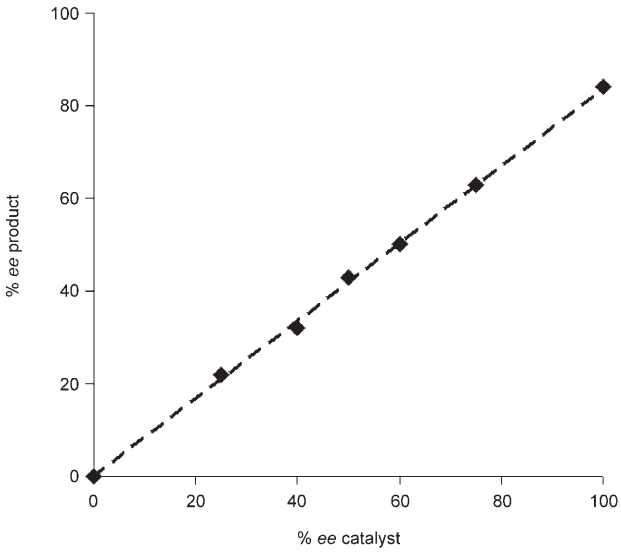

Figure 9. Linear relationship between *ee* of catalyst and product.

[**4a**] reveals that the reaction is first order in the alkene substrate [**4a**].

Next, plots of rate/[alkene] versus [aniline] for reactions carried out with three and four equivalents of aniline were produced (Figure 11), which once again demonstrates the inhibiting effect of the amine on reaction rate. However, significantly, the reaction progress data viewed over the course of a single reaction tell a different story. Even though these concentrations are not high enough to ensure pseudo-zero-order kinetics in aniline, Figure 11 shows that the rate of the reaction is independent of [aniline] over the course of the reaction, that is, the catalytic reaction displays overall zero order in aniline. This suggests that the detrimental effect of aniline on reaction turnover may be due to a decrease in the absolute concentration of active catalyst formed during the initial mixing of components, but that the instantaneous catalyst concentration during reaction turnover is not affected by [aniline].

Proposed catalytic cycle: Finally, a catalytic cycle for the palladium-catalysed aza-Michael reaction is constructed, which can account for all of the kinetic and spectroscopic observations (Scheme 8): Aniline premixed with the catalyst **1** and solvent in the reaction can form species **7** and **8**. At the beginning of the catalytic cycle, the imide substrate **4a** competes for vacant coordination sites at the dicationic metal centre to form complex **10**. The distribution is obviously dependent on the relative concentration of the two substrates. Formation of **10** is the slow step in the catalytic cycle, since the reaction is first order in **1** and **4a**, and that complex **1** was the major species observed during catalytic turnover. The nucleophilic attack of aniline on complex **10** and subsequent protonolysis steps are fast (zero order in aniline), leading to the formation of complex **11**. Product release is a reversible process, as established by the product inhibition study. Interestingly, since catalyst deactivation is

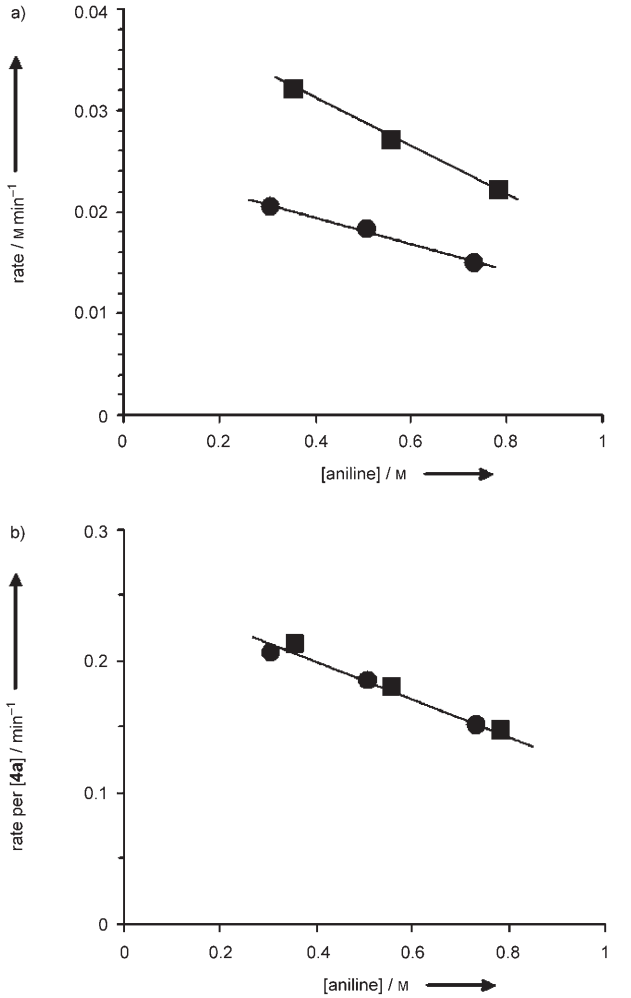

Figure 10. a) Reaction rate vs [aniline] at constant [**4a**] for data extracted from three separate reaction progress experiments; b) data from Figure 13a plotted as rate/[**4a**] vs [aniline]; concentrations: [**4a**]: ● 0.1 M, ■ 0.15 M.

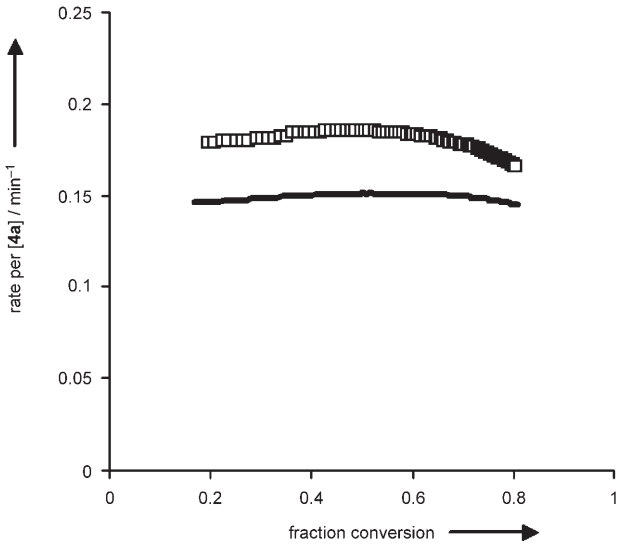

Figure 11. Plot of rate/[**4a**] vs fraction conversion at different excess of aniline: —— 4 equiv aniline, □ equiv aniline. Initial conditions: [**4a**] = 0.20 M, [**1**] = 0.043 M.

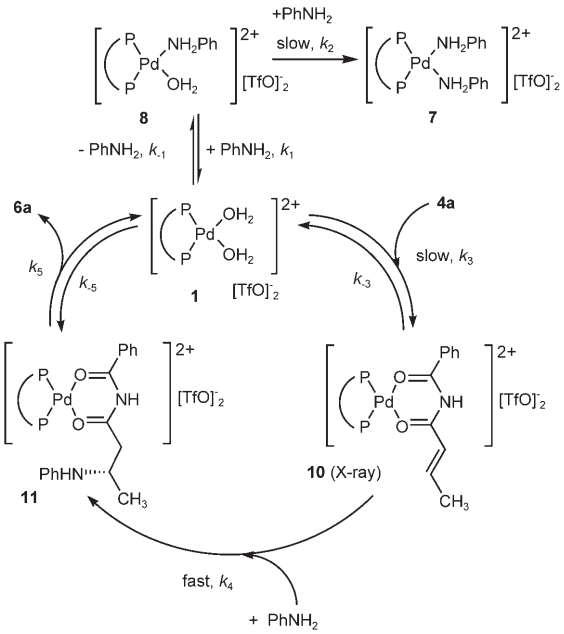

Scheme 8. Proposed catalytic cycle.

insignificant during the reaction, this implies that the formation of complex **10** (k_3) is much faster than that of **7** (k_2).

Improved reaction protocol: From the catalytic model established above, two important conclusions can be drawn: 1) The presence of excess amine at the beginning of the reaction controls the effective catalyst concentration; 2) The rate-limiting step precedes the stereo-defining step of the catalytic reaction, which is independent on the [aniline]. Therefore, by maintaining a low amine concentration over the course of the reaction, catalyst deactivation will be suppressed.

Thus, a new reaction protocol was devised, where the amine substrate is introduced slowly to a mixture of catalyst and **4a** via a syringe pump (over 20 h). The addition of 4-anisidine was chosen in this study, as this produced the worst results in previous studies. For comparison, catalytic reactions were also carried out at the same concentration using the "normal" protocol, that is, the entire amount of anisidine was added at the beginning of the reaction.

Gratifyingly, the new protocol does lead to significant improvements (Scheme 9). For the addition to **4a**, the *ee* was enhanced by more than 20% by using the new procedure. Similarly, for the addition to the *N*-carbamate substrate **20**, enhancement of both the yield and the enantioselectivity were achieved, the latter by nearly 30%.

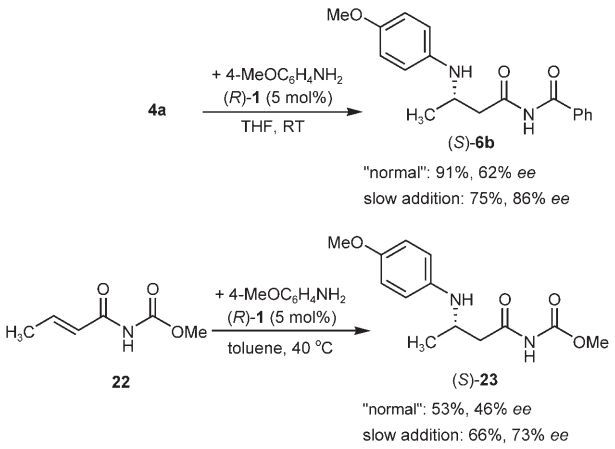

Scheme 9. Improving the reaction protocol.

Conclusion

Using complementary analytical tools, structural and kinetic aspects of the asymmetric aza-Michael reaction are delineated. During this investigation, important stereochemical aspects were uncovered, leading to the synthesis of optically active β^2- and $\beta^{2,3}$-amino acid derivatives. Reaction progress kinetic analysis revealed the important yet complex role played by the amine substrate. This led ultimately to the implementation of a new reaction protocol, which affords a significant enhancement of reaction yield and enantioselectivity.

Experimental Section

General methods: General synthetic and catalytic procedures have been previously described in publications from this research group.[1,2] All starting materials and reagents were used as received from commercial suppliers, unless noted otherwise. NMR samples were prepared in $CDCl_3$ unless otherwise indicated. Spectra were acquired using either a Jeol EX-270 instrument (^{1}H at 270 MHz, ^{31}P at 109.3 MHz and ^{13}C at 67.5 MHz), or a Bruker AVANCE 400 (^{1}H at 400 MHz, ^{31}P at 161.9 MHz and ^{13}C at 100.6 MHz) or 500 (^{1}H at 500 MHz and ^{13}C at 125.0 MHz) instruments. Chemical shifts (δ) are quoted in ppm, referenced to residual proton in $CDCl_3$ (7.27 ppm). UV-visible spectra were recorded using a Perkin Elmer Lambda 25 spectrometer and quartz cells (1 cm path length). Optical rotation values were obtained using a Perkin Elmer 343 Polarimeter using a 10 cm solution cell. Concentration of a sample is given in mg per mL. Calorimetric experiments were carried out using an OmniCal Calorimeter with WinCRC Super CRC software. HPLC analyses were performed on a Gilson system equipped with an autoinjector and a UV detector set at 254 nm.

Crystal data for 10: $[C_{55}H_{43}NO_2P_2Pd](CF_3SO_3)_2$, $M=1216.38$, orthorhombic, $P2_12_12_1$ (no. 19), $a=15.5234(12)$, $b=16.3999(15)$, $c=20.6530(19)$ Å, $V=5257.9(8)$ Å^3, $Z=4$, $\rho_{calcd}=1.537$ g cm^{-3}, $\mu(Cu_{K\alpha})=4.842$ mm^{-1}, $T=173$ K, yellow needles, Oxford Diffraction Xcalibur PX Ultra diffractometer; 10040 independent measured reflections, F^2 refinement, $R_1=0.042$, $wR_2=0.109$, 8852 independent observed absorption-corrected reflections [$|F_o| > 4\sigma(|F_o|)$, $2\theta_{max}=142°$], 776 parameters. The absolute structure of **10** was determined by a combination of *R* factor tests [$R_1^+=0.0424$, $R_1^-=0.0749$] and by use of the Flack parameter [$x^+=+0.003(7)$, $x^-=+0.997(7)$]. CCDC-622810 contains the supplementary crystallographic data for this paper. These data can be obtained free of charge from The Cambridge Crystallographic Data Centre via www.ccdc.cam.ac.uk/data_request/cif.

UV/Vis experiments: [((*R*)-BINAP)Pd(OH$_2$)$_2$][OTf]$_2$ (**1**) (2.1 mg, 2×10^{-3} mmol) was dissolved in THF (20 mL; 0.1 mM solution), whilst aniline (5.2 mg, 5.5×10^{-2} mmol) was dissolved in THF (5 mL; 11 mM solution). The solution of Pd complex **1** (3 mL) was placed in a UV quartz cuvette, and UV/Vis spectra were recorded, following the introduction of a known amount (0–3 equivalents) of the aniline solution using a microlitre syringe.

2-[D]-*N*-(But-2-enoyl)-benzamide (2-[D]-4a): DBU (1.50 mL, 9.95 mmol) and D_2O (5 mL) were added successively to a solution of the phosphonate imide $(EtO)_2P(O)CH_2CONHCOPh$[19] (3.0 g, 10.0 mmol) in $CDCl_3$ (10 mL) was added. The reaction mixture was stirred for 30 min, before the addition of acetaldehyde (0.45 g, 10.0 mmol). Upon completion of the reaction (TLC analysis), the reaction mixture was diluted with EtOAc (100 mL) and H_2O (50 mL). The layers were separated, and the aqueous portion extracted with additional EtOAc (100 mL). The combined organic extracts were washed with brine (50 mL), dried (Na_2SO_4) and the solvents were evaporated. The residue was purified by column chromatography to furnish the product as a white solid with 93% deuterium incorporation (0.67 g, 35%). $R_f=0.70$ (EtOAc/*n*-hexane 1:1); m.p. 110–111 °C; ^{1}H NMR (270 MHz, $CDCl_3$): δ = 8.76 (br s, 1H; NH), 7.91 (d, ^3J(H,H) = 7.8 Hz, 2H; ArH), 7.63 (t, ^3J(H,H) = 7.8 Hz, 1H; ArH), 7.51 (t, ^3J(H,H) = 7.8 Hz, 2H; ArH), 7.22 (q, ^3J(H,H) = 5.5 Hz, 1H; CH), 2.00 ppm (d, ^3J(H,H) = 5.5 Hz, 3H; CH_3); ^{13}C NMR (67.5 MHz, $CDCl_3$): δ = 167.6 (s), 166.0 (s), 147.0 (s), 133.2 (s), 133.0 (s), 128.9 (s), 127.9 (s), 124.6 (t, ^1J(C,D) = 24.8 Hz), 18.9 ppm (s); IR (KBr disc): $\tilde{\nu}_{max}=3233$, 1727, 1679, 1634, 1509 cm^{-1}; MS (EI): *m*/*z* (%): 190 (100) [M^+–H], 174 (20), 122 (20), 105 (78), 69 (98), 51 (28), 41 (29).

2-[D]-*N*-(3-Phenylaminobutyryl)-benzamide (2-[D]-6a): White solid. ^{1}H NMR (270 MHz, $CDCl_3$): δ = 9.13 (br s, 1H; NH), 7.74 (d, ^3J(H,H) = 7.4 Hz, 2H; ArH), 7.55 (t, *J* 7.4 Hz, 1H; ArH), 7.37 (t, ^3J(H,H) = 7.4 Hz, 2H; ArH), 7.00 (t, ^3J(H,H) = 8.4 Hz, 2H; ArH), 6.59 (t, ^3J(H,H) = 8.4 Hz, 1H; ArH), 6.52 (d, ^3J(H,H) = 8.4 Hz, 2H; ArH), 4.00–4.09 (m, 1H; CHN), 3.79 (br s, 1H; NH), 3.10 (br d, ^3J(H,H) = 5.7 Hz, 1H; CHD), 1.27 ppm (d, ^3J(H,H) = 6.7 Hz, 3H; CH_3); MS (EI): *m*/*z* (%): 283 (20) [M^+–H], 120 (100), 105 (28), 77 (30).

***N*-(2-Methylacryloyl)-benzamide (12)**: EtMgBr (1M in THF, 19.4 mL, 19.4 mmol) was added to a stirred solution of methacrylamide (1.50 g, 17.6 mmol) in THF (20 mL) at −20 °C. After 1 h, benzoyl chloride (3.1 mL, 26.7 mmol) was added and the reaction mixture was stirred for 2 h, then at room temperature for another hour. The reaction was quenched by the addition of saturated aq. NH_4Cl (10 mL), then extracted with EtOAc (3×10 mL). The combined organic layers were washed with water (20 mL) and brine (20 mL), dried (Na_2SO_4) and evaporated under reduced pressure. The residue was purified by column chromatography to give the product as a white solid (1.34 g, 40%). $R_f=0.53$ (EtOAc/*n*-hexane 1:1); m.p. 71–72 °C; ^{1}H NMR (270 MHz, $CDCl_3$): δ = 9.18 (br s, 1H; NH), 7.77 (d, ^3J(H,H) = 7.4 Hz, 2H; ArH), 7.51 (t, ^3J(H,H) = 7.4 Hz, 1H; ArH), 7.39 (t, ^3J(H,H) = 7.4 Hz, 2H; ArH), 5.82 (s, 1H; =CH_2), 5.55 (s, 1H; =CH_2), 1.97 ppm (s, 3H; CH_3); ^{13}C NMR (67.5 MHz, $CDCl_3$): δ = 167.5 (s), 166.4 (s), 140.0 (s), 133.2 (s), 132.7 (s), 128.5 (s), 127.8 (s), 122.0 (s), 18.2 ppm (s); IR (KBr disc): $\tilde{\nu}_{max}=3255$, 1703, 1674, 1634, 1481 cm^{-1}; MS (EI): *m*/*z* (%): 189 (100) [M^+–H], 174 (30), 122 (25), 105 (74), 69 (98), 51 (28), 41 (29); elemental analysis calcd (%) for $C_{11}H_{11}NO_2$: C 69.83, H 5.86, N 7.40; found C, 69.72, H 5.82, N 7.32.

***N*-(2-Methylacryloyl)-carbamic acid methyl ester (13)**: Oxalyl chloride (22.3 mL, 0.26 mol) and a drop of DMF were added to a solution of methacrylic acid (20 mL, 0.24 mol) in dry CH_2Cl_2 (50 mL). The reaction mixture was stirred for 2 h, after which the volatile components were evaporated to leave methacryloyl chloride as an oily residue. In a separate flask, a solution of methyl carbamate (3.59 g, 47.8 mmol) in THF (10 mL) was added to a suspension of NaH (60% in paraffin, 2.9 g, 71.8 mmol) in dry THF (120 mL) at 0 °C. Stirring was continued for 30 min, before the addition of methacryloyl chloride (7.50 g, 71.8 mmol). The reaction mixture was stirred at ambient temperature for another 2 h, before it was quenched by the addition of 1N aq. HCl (100 mL). The

mixture was extracted with CH_2Cl_2 (3×100 mL), and the combined organic layers were washed with aq. $NaHCO_3$ (3×50 mL), dried over $MgSO_4$, evaporated and purified by flash column chromatography. The product was obtained as a white solid (1.64 g, 24%). R_f=0.35 (Et_2O); m.p. 92–93 °C; ^{1}H NMR (270 MHz, $CDCl_3$): δ = 8.44 (brs, 1H, NH), 5.80 (s, 1H; =CH_2), 5.51 (s, 1H; =CH_2), 3.70 (s, 3H; OCH_3), 1.97 ppm (s, 3H; CH_3); ^{13}C NMR (100.6 MHz, $CDCl_3$): δ = 166.0 (s), 151.7 (s), 139.3 (s), 122.1 (s), 52.6 (s), 18.1 ppm (s); IR (KBr disc): $\tilde{\nu}_{max}$=3286, 3108, 3002, 2958, 1773, 1687, 1636, 1458, 1225 cm^{-1}; MS (EI): *m*/*z* (%): 143 (45) [M^+−H], 115 (14), 100 (24), 69 (82), 68 (48), 59 (26); elemental analysis calcd (%) for $C_6H_9NO_3$: C 50.35, H 6.34, N 9.79, found: C 50.43, H 6.24, N 9.65.

Similar procedures were used for the preparation of tigloyl derivatives **14** and **15**.

***N*-(2-Methylbut-2-enoyl)-benzamide (14)**:[14] The product was obtained as a white solid in 40% yield. R_f=0.60 (Et_2O); m.p. 103–104 °C; ^{1}H NMR (400 MHz, $CDCl_3$): δ = 8.80 (brs, 1H; NH), 7.81 (d, ^3J(H,H)=7.4 Hz, 2H; ArH), 7.58 (t, ^3J(H,H)=7.4 Hz, 1H; ArH), 7.47 (t, ^3J(H,H)=7.4 Hz, 2H; ArH), 6.60 (q, ^3J(H,H)=6.8 Hz, 1H; CH), 1.92 (s, 3H; CH_3), 1.85 ppm (d, ^3J(H,H)=6.8 Hz, 3H; CH_3); ^{13}C NMR (100.6 MHz, $CDCl_3$): δ = 168.2 (s), 166.6 (s), 134.8 (s), 134.1 (s), 133.6 (s), 133.0 (s), 128.8 (s), 127.8 (s), 14.4 (s), 12.4 ppm (s); IR (KBr disc): $\tilde{\nu}_{max}$=3270, 1692, 1674, 1600, 1481 cm^{-1}; MS (EI): *m*/*z* (%): 203 (32) [M^+−H], 188 (20), 105 (100), 83 (31), 55 (48).

***N*-(2-Methylbut-2-enoyl)-carbamic acid methyl ester (15)**: The product was obtained as a white solid in 26% yield. R_f=0.32 (Et_2O); m.p. 107–108 °C; ^{1}H NMR (400 MHz, $CDCl_3$): δ = 7.80 (brs, 1H; NH), 6.53 (q, ^3J(H,H)=6.8 Hz, 1H; CH), 3.81 (s, 3H; OCH_3), 1.89 (s, 3H; CH_3), 1.83 ppm (d, ^3J(H,H)=6.8 Hz, 3H; CH_3); ^{13}C NMR (100.6 MHz, $CDCl_3$): δ = 166.5 (s), 151.8 (s), 134.2 (s), 131.9 (s), 52.7 (s), 14.2 (s), 12.0 ppm (s); IR (KBr disc): $\tilde{\nu}_{max}$=3290, 1745, 1682, 1513, 1460, 1214 cm^{-1}; MS (EI): *m*/*z* (%): 157 (72) [M^+−H], 129 (12), 83 (66), 82 (100), 55 (81), 54 (43); elemental analysis calcd (%) for $C_7H_{11}NO_3$: C 53.49, H 7.05, N 8.91, found: C 53.33, H 6.95, N 8.85.

(*S*)-(−)-*N*-[3-(4-Chlorophenylamino)-2-methylpropionyl]-benzamide (16a): White solid. R_f=0.57 (EtOAc/pet. ether 40–60 1:1); m.p. 152–153 °C; chiral HPLC (Chiralcel AD, 254 nm, 10% isopropylalcohol (IPA) in hexane, 1 mL min^{-1}): t_R(minor)=23.7 min, t_R(major)=28.3 min; $[\alpha]_D^{23}$=−13.4° (78% *ee*, *c*=1.00 in $CHCl_3$); ^{1}H NMR (270 MHz, $CDCl_3$): δ = 9.16 (brs, 1H; NH), 7.81 (d, ^3J(H,H)=7.4 Hz, 2H; ArH), 7.58 (t, ^3J(H,H)=7.4 Hz, 1H; ArH), 7.45 (t, ^3J(H,H)=7.4 Hz, 2H; ArH), 7.09 (d, ^3J(H,H)=8.9 Hz, 2H; ArH), 6.54 (d, ^3J(H,H)=8.9 Hz, 2H; ArH), 4.19 (brs, 1H; NH), 3.78–3.90 (m, 1H; CH), 3.50 (dd, ^3J(H,H)=8.4, ^2J(H,H)=12.8 Hz, 1H; CH_2), 3.24 (dd, ^3J(H,H)=4.9, ^2J(H,H)=12.8 Hz, 1H; CH_2), 1.30 ppm (d, ^3J(H,H)=6.9 Hz, 3H, CH_3); ^{13}C NMR (67.5 MHz, $CDCl_3$): δ=178.0 (s), 165.5 (s), 146.3 (s), 133.3 (s), 132.6 (s), 129.1 (s), 128.9 (s), 127.7 (s), 122.2 (s), 114.1 (s), 47.0 (s), 40.2 (s), 15.0 ppm (s); IR (KBr): $\tilde{\nu}_{max}$=3368, 3255, 1726, 1681, 1601, 1502, 819, 710 cm^{-1}; MS (EI): *m*/*z* (%): 318/317 (10/5) [M^+−H], 316 (23), 177 (46), 154 (100), 142 (28), 140 (100), 105 (98), 77 (54), 45 (47); elemental analysis calcd (%) for $C_{17}H_{17}ClN_2O_2$: C 64.46, H 5.41, N 8.84, found: C 64.36, H 5.37, N 8.77.

(*S*)-(−)-*N*-(2-Methyl-3-phenylaminopropionyl)-benzamide (16b): White solid; R_f=0.57 (EtOAc/pet. ether 40–60 1:1); m.p. 139–140 °C; chiral HPLC (Chiralpak AD, 254 nm, 10% IPA in hexane, 1 mL min^{-1}): t_R(minor)=20.4 min, t_R(major)=35.8 min; $[\alpha]_D^{23}$=−12.8° (77% *ee*, *c*=1.00 in $CHCl_3$); ^{1}H NMR (270 MHz, $CDCl_3$): δ = 9.11 (brs, 1H; NH), 8.13 (d, ^3J(H,H)=7.4 Hz, 2H; ArH), 7.81 (t, ^3J(H,H)=7.4 Hz, 1H; ArH), 7.51 (t, ^3J(H,H)=7.4 Hz, 2H; ArH), 7.18 (t, ^3J(H,H)=8.4 Hz, 2H; ArH), 6.74 (t, ^3J(H,H)=8.4 Hz, 1H; ArH), 6.68 (d, ^3J(H,H)=8.4 Hz, 2H; ArH), 3.79–3.86 (m, 1H; CH), 3.79 (brs, 1H; NH), 3.56 (dd, ^3J(H,H)=8.6, ^2J(H,H)=12.8 Hz, 1H; CH_2), 3.33 (dd, ^3J(H,H)=4.7, ^2J(H,H)=12.8 Hz, 1H; CH_2), 1.34 ppm (d, ^3J(H,H)=6.9 Hz, 3H; CH_3); ^{13}C NMR (67.5 MHz, $CDCl_3$): δ=177.8 (s), 166.0 (s), 147.5 (s), 133.7 (s), 132.8 (s), 129.4 (s), 128.9 (s), 127.7 (s), 118.1 (s), 113.2 (s), 47.1 (s), 40.4 (s), 15.0 ppm (s); IR (KBr disc): $\tilde{\nu}_{max}$=3372, 3268, 1725, 1691, 1603, 1504, 805 cm^{-1}; MS (EI): *m*/*z* (%): 282 (19) [M^+−H], 120 (100), 105 (23), 77 (31); elemental analysis calcd (%) for $C_{17}H_{18}N_2O_2$: C 72.32, H 6.43, N 9.92, found: C 72.21, H 6.42, N 9.91.

(*S*)-(−)-*N*-[3-(4-Methoxylphenylamino)-2-methyl-propionyl]-benzamide (16c): White solid; R_f=0.31 (EtOAc/pet. ether 40–60 1:1); m.p. 134–135 °C; chiral HPLC (Chiralpak AD, 254 nm, 10% IPA in hexane, 1 mL min^{-1}): t_R(minor)=34.9 min, t_R(major)=49.6 min; $[\alpha]_D^{23}$=−3.3° (45% *ee*, *c*=1.00 in $CHCl_3$); ^{1}H NMR (270 MHz, $CDCl_3$): δ=9.28 (brs, 1H; NH), 7.77 (d, ^3J(H,H)=7.4 Hz, 2H; ArH), 7.57 (t, ^3J(H,H)=7.4 Hz, 1H; ArH), 7.43 (t, ^3J(H,H)=7.4 Hz, 2H; ArH), 6.79 (d, ^3J(H,H)=8.9 Hz, 2H; ArH), 6.65 (d, ^3J(H,H)=8.9 Hz, 2H; ArH), 3.83 (brs, 1H; NH), 3.74 (s, 3H; OCH_3), 3.59–3.71 (m, 1H; CH), 3.50 (dd, ^3J(H,H)=8.6, ^2J(H,H)=12.6 Hz, 1H; CH_2N), 3.28 (dd, ^3J(H,H)=4.5, ^2J(H,H)=12.6 Hz, 1H; CH_2N), 1.32 ppm (d, ^3J(H,H)=6.9 Hz, 3H, CH_3); ^{13}C NMR (67.5 MHz, $CDCl_3$): δ=176.9 (s), 165.5 (s), 152.8 (s), 141.6 (s), 133.1 (s), 132.9 (s), 128.9 (s), 127.6 (s), 115.0 (s), 112.9 (s), 55.8 (s), 48.3 (s), 40.5 (s), 14.8 ppm (s); IR (KBr disc): $\tilde{\nu}_{max}$=3368, 3273, 1728, 1673, 1600, 1485, 1234, 823 cm^{-1}; MS (EI): *m*/*z* (%): 312 (31) [M^+−H], 136 (100), 105 (38), 77 (25), 44 (35); elemental analysis calcd (%) for $C_{18}H_{20}N_2O_3$: C 69.21, H 6.45, N 8.97, found: C 69.16, H 6.37, N 8.86.

(*S*)-(−)-[3-(4-Chlorophenylamino)-2-methylpropionyl]-carbamic acid methyl ester (17a): White solid; m.p. 124–125 °C; R_f=0.67 (Et_2O); chiral HPLC (Chiralcel OD-H, 254 nm, 5% IPA in hexane, 1 mL min^{-1}): t_R-(minor)=31.0 min, t_R(major)=41.7 min; $[\alpha]_D^{23}$=−21.8° (81% *ee*, *c*=1.00 in $CHCl_3$); ^{1}H NMR (270 MHz, $CDCl_3$): δ=7.61 (brs, 1H; NH), 7.11 (d, ^3J(H,H)=8.6 Hz, 2H; ArH), 6.53 (d, ^3J(H,H)=8.6 Hz, 2H; ArH), 4.00 (brs, 1H, NH), 3.76 (s, 3H; OCH_3), 3.41–3.51 (m, 2H; CH_2N, CH), 3.20 (dd, ^3J(H,H)=4.2, ^2J(H,H)=12.8 Hz, 1H; CH_2N), 1.24 ppm (d, ^3J(H,H)=6.4 Hz, 3H, CH_3); ^{13}C NMR (125.0 MHz, $CDCl_3$): δ=176.2 (s), 151.9 (s), 146.3 (s), 129.1 (s), 122.3 (s), 114.1 (s), 53.2 (s), 46.8 (s), 39.3 (s), 15.2 ppm (s); IR (KBr disc): $\tilde{\nu}_{max}$=3388, 3221, 1768, 1679, 1601, 1510, 1215, 812, 718 cm^{-1}; MS (EI): *m*/*z* (%): 272/271 (7/2) [M^+−H], 270 (17), 238 (18), 142 (41), 140 (100); elemental analysis calcd (%) for $C_{12}H_{15}ClN_2O_3$: C 53.24, H 5.58, N 10.35, found: C 53.34, H 5.68, N 10.38.

(*S*)-(−)-*N*-(2-Methyl-3-phenylaminopropionyl)-carbamic acid methyl ester (17b): White solid; m.p. 110–111 °C; R_f=0.67 (Et_2O); chiral HPLC (Chiralpak AD, 254 nm, 2% IPA in hexane, 1 mL min^{-1}): t_R(minor)=37.1 min, t_R(major)=41.5 min; $[\alpha]_D^{23}$=−19.1° (85% *ee*, *c*=1.00 in $CHCl_3$); ^{1}H NMR (270 MHz, $CDCl_3$): δ=7.26 (brs, 1H; NH), 7.18 (t, ^3J(H,H)=7.9 Hz, 2H; ArH), 6.72 (t, ^3J(H,H)=7.9 Hz, 1H; ArH), 6.63 (d, ^3J(H,H)=7.9 Hz, 2H; ArH), 4.00 (brs, 1H; NH), 3.76 (s, 3H; OCH_3), 3.46–3.49 (m, 2H; CH_2N, CH), 3.25 (dd, ^3J(H,H)=4.2, ^2J(H,H)=12.8 Hz, 1H; CH_2), 1.25 ppm (d, ^3J(H,H)=6.2 Hz, 3H, CH_3); ^{13}C NMR (125.0 MHz, $CDCl_3$): δ=176.1 (s), 151.9 (s), 147.6 (s), 129.3 (s), 117.9 (s), 113.1 (s), 53.1 (s), 46.9 (s), 39.6 (s), 15.1 ppm (s); IR (KBr disc): $\tilde{\nu}_{max}$=3248, 3172, 1763, 1688, 1605, 1517, 787 cm^{-1}; MS (EI): *m*/*z* (%): 236 (12) [M^+−H], 204 (10), 119 (10), 106 (100), 77 (11); elemental analysis calcd (%) for $C_{12}H_{16}N_2O_3$: C 61.00, H 6.83, N 11.86; found: C 61.00, H 6.82, N 11.85.

(*S*)-(−)-*N*-[3-(4-Methoxylphenylamino)-2-methylpropionyl]-carbamic acid methyl ester (17c): White solid; m.p. 102–103 °C; R_f=0.53 (Et_2O); chiral HPLC (Chiralcel OD-H, 254 nm, 5% IPA in hexane, 1 mL min^{-1}): t_R(minor)=56.7 min, t_R(major)=68.6 min; $[\alpha]_D^{23}$=−1.00° (45% *ee*, *c*=1.00 in $CHCl_3$); ^{1}H NMR (270 MHz, $CDCl_3$): δ = 8.35 (brs, 1H; NH), 6.79 (d, ^3J(H,H)=8.6 Hz, 2H; ArH), 6.75 (d, ^3J(H,H)=8.6 Hz, 2H; ArH), 4.00 (brs, 1H; ArH), 3.74 (s, 6H; 2×OCH_3), 3.30–3.40 (m, 2H; CH_2N, CH), 3.18 (dd, ^3J(H,H)=4.2, ^2J(H,H)=12.8 Hz, 1H; CH_2N), 1.22 ppm (d, ^3J(H,H)=6.7 Hz, 3H; CH_3); ^{13}C NMR (125.0 MHz, $CDCl_3$): δ=175.9 (s), 165.7 (s), 152.8 (s), 141.7 (s), 116.5 (s), 114.8 (s), 55.8 (s), 53.0 (s), 48.2 (s), 39.8 (s), 15.0 ppm (s); IR (KBr disc): $\tilde{\nu}_{max}$=3261, 3180, 1762, 1688, 1513, 1230, 816 cm^{-1}; MS (EI): *m*/*z* (%): 266 (15) [M^+−H], 234 (25), 143 (32), 136 (91), 123 (27), 108 (38), 69 (72); elemental analysis calcd (%) for $C_{13}H_{18}N_2O_4$: C 58.63, H 6.81, N 10.52, found: C 58.72 H, 6.75, N 10.44.

(*S*)-(+)-3-Amino-2-methylpropionyl-benzamide [(*S*)-(+)-18]: A solution of ceric ammonium nitrate (1.58 g, 2.88 mmol) in H_2O (17 mL) was added dropwise to a solution of (−)-**16c** (200 mg, 0.64 mmol, 45% *ee*) in MeCN/H_2O (22 mL:5 mL) at −10 °C. After 1 h, the reaction was quenched by the addition of saturated sodium sulfite solution (15 mL),

and the mixture was then extracted with EtOAc (3×40 mL). The combined organic layers were then extracted with 1 N HCl (50 mL). Following separation, the aqueous phase was neutralised with $NaHCO_3$ and extracted further with EtOAc (3×40 mL). Finally, the combined organic layers were washed with brine, dried ($MgSO_4$) and evaporated to afford **19** (120 mg, 91%). $[\alpha]_D^{23}=+6.6°$ (45% *ee*, $c=1.00$ in $CHCl_3$); ^{1}H NMR (400 MHz, $CDCl_3$): δ = 9.77 (brs, 1H; NH), 7.80 (d, $^3J(H,H)=7.3$ Hz, 2H; ArH), 7.50 (t, $^3J(H,H)=7.3$ Hz, 1H; ArH), 7.40 (t, $^3J(H,H)=7.3$ Hz, 2H; ArH), 3.60–3.70 (m, 1H; CH), 3.50 (dd, $^3J(H,H)=8.6$ Hz, 12.6, 1H; CH_2), 3.28 (dd, $^3J(H,H)=4.5$, $^2J(H,H)=12.6$ Hz, 1H; CH_2), 2.00 (brs, 2H; NH_2), 1.32 ppm (d, $^3J(H,H)=6.9$ Hz, 3H, CH_3); ^{13}C NMR (100.6 MHz, $CDCl_3$): $\delta=173.0$ (s), 165.0 (s), 134.0 (s), 132.5 (s), 128.5 (s), 128.7 (s), 48.5 (s), 43.5 (s), 21.9 ppm (s); MS (EI): *m*/*z* (%): 206 (100) [M^+−H], 143 (32), 136 (9), 123 (7), 108 (38), 69 (72); elemental analysis calcd (%) for $C_{11}H_{14}N_2O_2$: C 64.06, H 6.84, N 13.58, found C, 64.10, H 6.73, N 13.51.

(*S*)-(+)-3-Amino-2-methylpropanoic acid (β²-alanine) [(*S*)-(+)-19]: (*S*)-(+)-**18** (70 mg, 0.34 mmol, 45% *ee*) was hydrolysed by stirring with 1 N KOH in MeOH (5 mL) at room temperature for one hour, after which the solvents were evaporated. The residue was dissolved in H_2O (5 mL), and washed with portions of Et_2O (3×5 mL). The pH of the aqueous layer was adjusted to 4 by the addition of 1 N HCl, before it was extracted with EtOAc (4×10 mL). Finally, the combined organic layers were washed with brine, dried ($MgSO_4$) and evaporated to afford (*S*)-(+)-**19** (35 mg, 100%). $[\alpha]_D^{23}=+4.9°$ ($c=0.3$ in 1 N HCl, 45% *ee*), (lit.[13] +11.0°, $c=0.3$ in 1 N HCl, (*S*)-enantiomer); ^{1}H NMR (400 MHz, $CDCl_3$): $\delta=6.50$ (brs, 1H; OH), 3.08 (dd, $^3J(H,H)=8.4$, $^2J(H,H)=12.8$ Hz, 1H; CH_2), 2.98 (dd, $^3J(H,H)=5.3$, $^2J(H,H)=12.8$ Hz, 1H; CH_2), 2.58 (m, 1H; CH), 2.00 (brs, 2H; NH_2), 1.13 ppm (d, $^3J(H,H)=6.4$ Hz, 3H; CH_3); ^{13}C NMR (100.6 MHz, $CDCl_3$): $\delta=177.6$ (s), 41.5 (s), 37.6 (s), 14.1 ppm (s).

(−)-*N*-[3-(4-Chlorophenylamino)-2-methylbutyryl]-benzamide (20): White solid; m.p. 170–171 °C; $R_f=0.63$ (EtOAc/*n*-hexane 1:1); chiral HPLC (Chiralcel OD-H, 254 nm, 5% IPA in hexane, 1 mL min^{-1}): t_R-(major)=25.9, t_R(minor)=44.0 min; $[\alpha]_D^{23}=-20.0°$ (53% *ee*, $c=1.00$ in $CHCl_3$); ^{1}H NMR (400 MHz, $CDCl_3$): $\delta=9.12$ (brs, 1H; NH), 7.77 (d, $^3J(H,H)=7.3$ Hz, 2H; ArH), 7.61 (t, $^3J(H,H)=7.3$ Hz, 1H; ArH), 7.47 (t, $^3J(H,H)=7.3$ Hz, 2H; ArH), 7.16 (d, $^3J(H,H)=8.8$ Hz, 2H; ArH), 6.63 (d, $^3J(H,H)=8.8$ Hz, 2H; ArH), 4.20 (brs, 1H; NH), 3.87 (quintet, $^3J(H,H)=6.9$ Hz, 1H; CHCO), 3.80 (quintet, $^3J(H,H)=6.4$ Hz, 1H; CHN), 1.34 (d, $^3J(H,H)=6.9$ Hz, 3H; CH_3), 1.31 ppm (d, $^3J(H,H)=6.4$ Hz, 3H; CH_3); ^{13}C NMR (100.6 MHz, $CDCl_3$): $\delta=178.0$ (s), 165.5 (s), 146.3 (s), 133.0 (s), 132.5 (s), 129.0 (s), 128.8 (s), 127.8 (s), 122.0 (s), 114.9 (s), 53.3 (s), 45.3 (s), 15.5 (s), 12.1 ppm (s); IR (KBr disc): $\tilde{\nu}_{max}=3368$, 3255, 1726, 1681, 1601, 1502, 819, 710 cm^{-1}; MS (EI): *m*/*z* (%): 332/331 (4/2) [M^+−H], 330 (10), 154 (100), 105 (18), 77 (15); elemental analysis calcd (%) for $C_{18}H_{19}ClN_2O_2$: C 65.35, H 5.791, N 8.47, found: C 65.30, H 5.75, N 8.40.

(−)-[3-(4-Chlorophenylamino)-2-methylbutyryl]-carbamic acid methyl ester (21): White solid; m.p. 166–167 °C; $R_f=0.38$ (EtOAc/*n*-hexane 1:1); chiral HPLC (Chiralpak AD, 254 nm, 5% IPA in hexane, 1 mL min^{-1}): t_R-(minor)=24.9 min, t_R(major)=30.1 min; $[\alpha]_D^{23}=-0.4°$ (83% *ee*, $c=1.00$ in $CHCl_3$); ^{1}H NMR (400 MHz, $CDCl_3$): $\delta=7.29$ (brs, 1H; NH), 7.17 (d, $^3J(H,H)=8.8$ Hz, 2H; ArH), 6.60 (d, $^3J(H,H)=8.8$ Hz, 2H; ArH), 3.79 (s, 3H; OCH_3), 3.69–3.70 (m, 2H; CH, NH), 3.20 (m, 1H; CH), 1.28 (d, $^3J(H,H)=7.1$ Hz, 3H; CH_3), 1.26 ppm (d, $^3J(H,H)=6.5$ Hz, 3H; CH_3); ^{13}C NMR (100.6 MHz, $CDCl_3$): $\delta=174.0$ (s), 151.5 (s), 145.2 (s), 129.3 (s), 123.2 (s), 115.1 (s), 53.0 (s), 51.7 (s), 44.4 (s), 17.7 (s), 13.2 ppm (s); IR (KBr disc): $\tilde{\nu}_{max}=3387$, 3290, 1777, 1697, 1604, 1501, 1237, 814, 718 cm^{-1}; MS (EI): *m*/*z* (%): 286/285 (28/12) [M^+−H], 284 (78), 252 (41), 237 (10), 194 (21), 154 (100); elemental analysis calcd (%) for $C_{13}H_{17}ClN_2O_3$: C 54.84, H 6.02, N 9.84, found: C 54.97, H 5.93, N 9.96.

Calorimetric experiment: A reaction vessel was charged with a mixture of *N*-but-2-enoyl benzamide **4a**, aniline and dry THF (2 mL). This was placed in the calorimeter and stirred at 31 °C. Meanwhile, a syringe containing a solution of Pd complex **1** in THF (0.5 mL) was placed in the injection port of the calorimeter. When thermal equilibrium was established (ca. 1 h), the catalyst solution was injected, giving rise to a detectable heat flow which was recorded. Kinetic parameters were determined by fitting the reaction rate data obtained from the heat flow to an analytical rate equation using the Solver program in Excel (Microsoft). Non-linear statistical analysis for about 2650 total data points were carried out. At the end of the reaction, a sample of the reaction was collected via syringe and injected into a solution of Et_2O/H_2O 1:1. The organic layer was extracted, evaporated and the residue was analysed using NMR and chiral HPLC.

Slow addition method: To a mixture of **4a** (300 mg, 1.59 mmol) and complex **1** (78 mg, 0.07 mmol) in THF (15 mL), a solution of *p*-anisidine (180 mg, 1.44 mmol) in THF (5 mL) was added slowly using a syringe pump at a rate of 0.25 mL min^{-1} (over 20 h). The reaction mixture was evaporated, and the residue was re-dissolved in diethyl ether and passed through a short pad of silica. The conversion and *ee* were determined by NMR and chiral HPLC analyses. For comparison, the reaction was repeated under the same conditions, except anisidine was added in one portion at the beginning of the reaction.

[3-(4-Methoxylphenylamino)-butyryl]-carbamic acid methyl ester (23): White solid; m.p. 89–90 °C; $R_f=0.31$ (Et_2O/pentane 1:1); chiral HPLC (Chiralcel OD-H, 254 nm, 5% IPA in hexane, 1 mL min^{-1}): t_R(major)=52.2 min, t_R(minor)=71.2 min; $[\alpha]_D^{23}=-6.3°$ (60% *ee*, $c=1.00$ in $CHCl_3$); ^{1}H NMR (270 MHz, $CDCl_3$): $\delta=8.14$ (brs, 1H; NH), 6.78 (d, $^3J(H,H)=8.9$ Hz, 2H; ArH), 6.64 (d, $^3J(H,H)=8.9$ Hz, 2H; ArH), 4.00 (brs, 1H; NH), 3.79–3.93 (m, 1H; CH), 3.75 (s, 3H; OCH_3), 3.74 (s, 3H; OCH_3), 2.95 (dd, $^3J(H,H)=6.4$, $^2J(H,H)=16.1$ Hz, 1H; CH_2), 2.81 (dd, $^3J(H,H)=6.4$, $^2JH,H)=16.1$ Hz, 1H; CH_2), 1.26 ppm (d, $^3J(H,H)=6.4$ Hz, 3H; CH_3); ^{13}C NMR (125.0 MHz, $CDCl_3$): δ = 172.3 (s), 152.9 (s), 152.1 (s), 140.5 (s), 116.2 (s), 114.8 (s), 55.6 (s), 53.0 (s), 47.6 (s), 42.3 (s), 20.8 ppm (s); IR (KBr disc): $\tilde{\nu}_{max}=3354$, 3270, 1768, 1705, 1511, 1467, 1235, 824 cm^{-1}; MS (EI): *m*/*z* (%): 266 (30) [M^+−H], 234 (13), 193 (8), 176 (14), 150 (100), 149 (10), 134 (15), 69 (59); elemental analysis calcd (%) for $C_{13}H_{18}N_2O_4$: C 58.63, H 6.81, N 10.52, found: C 58.76, H 6.96, N 10.63.

Acknowledgements

Part of this work was conducted at DSM's research facility in Geleen (August–October 2005). Their generosity and hospitality is much appreciated. We are also grateful to the Committee of Vice-Chancellors and Principals (CVCP) for an ORS award (to P.H.P.), DSM and Imperial College for additional studentship support, and Johnson Matthey for the loan of Pd salts.

[1] a) K. Li, K. K. Hii, *Chem. Commun.* **2003**, 1132–1133; b) K. Li, X. Cheng, K. K. Hii, *Eur. J. Org. Chem.* **2004**, 959–964; c) P. H. Phua, J. G. de Vries, K. K. Hii, *Adv. Synth. Catal.* **2005**, *347*, 1775–1780.

[2] P. H. Phua, J. G. de Vries, K. K. Hii, *Adv. Synth. Catal.* **2006**, *348*, 587–592.

[3] Y. Hamashima, H. Somei, Y. Shimura, T. Tamura, M. Sodeoka, *Org. Lett.* **2004**, *6*, 1861–1864.

[4] THF has been previously shown to be a good substitute for toluene for this reaction, see ref. [1c].

[5] U. Anandhi, T. Holbert, S. Lueng, P. R. Sharp, *Inorg. Chem.* **2003**, *42*, 1282–1295.

[6] D. Nama, D. Schott, P. S. Pregosin, L. F. Veiros, M. J. Calhorda, *Organometallics* **2006**, *25*, 4596–4604.

[7] J. Vicente, A. Arcas, *Coord. Chem. Rev.* **2005**, *249*, 1135–1154.

[8] P. J. Stang, D. H. Cao, G. T. Poulter, A. M. Arif, *Organometallics* **1995**, *14*, 1110–1114.

[9] R. K. Poole, C. L. Bashford, in *Spectrophotometry and Spectrofluorimetry: A Practical Approach* (Eds.: D. A. Harris, C. L. Bashford), IRL Press, Oxford, **1987**, pp. 23–489.

[10] Complexes **9** and **9′** can be generated by the addition of aniline to μ-hydroxy complex **5**, see reference [6].

[11] $[Pd(\mu\text{-}OH)(BINAP)]_2[CF_3SO_3]_2$ **5** deprotonates the acidic NH moiety of alkenoyl–*N*-imide, which forms a chelate ring with Pd to

give a monocationic complex: P. S. Pregosin, A. Albinati, S. Rizzato, unpublished results.
[12] At higher temperatures, competitive acyl substitution occurs.
[13] C. Agami, S. Cheramy, L. Dechoux, M. Melaimi, *Tetrahedron* **2001**, *57*, 195–200.
[14] M. P. Sibi, N. Prabagaran, S. G. Ghorpade, C. P. Jasperse, *J. Am. Chem. Soc.* **2003**, *125*, 11796–11797.
[15] The relative stereochemistry of the diastereomer cannot be established by ^{1}H NMR correlations due to fast C–C bond rotation, even at −60 °C.
[16] For reviews on the concepts of reaction progress kinetic analysis, see: a) J. S. Mathew, M. Klussmann, H. Iwamura, F. Valera, A. Futran, E. A. C. Emanuelsson, D. G. Blackmond, *J. Org. Chem.* **2006**, *71*, 4711–4722; b) D. G. Blackmond, *Angew. Chem.* **2005**, *117*, 4374–4393; *Angew. Chem. Int. Ed.* **2005**, *44*, 4302–4320.
[17] a) T. Rosner, J. Le Bars, A. Pfaltz, D. G. Blackmond, *J. Am. Chem. Soc.* **2001**, *123*, 1848–1855; b) U. K. Singh, E. R. Strieter, D. G. Blackmond, S. L. Buchwald, *J. Am. Chem. Soc.* **2002**, *124*, 14104–14114; c) L. C. P. Nielsen, C. P. Stevenson, D. G. Blackmond, E. N. Jacobsen, *J. Am. Chem. Soc.* **2004**, *126*, 1360–1362.
[18] M. Klussmann, S. P. Mathew, H. Iwamura, D. H. Wells, Jr., A. Armstrong, D. G. Blackmond, *Angew. Chem.* **2006**, *118*, 8157–8160; *Angew. Chem. Int. Ed.* **2006**, *47*, 7989–7992.
[19] S. N. Goodman, E. N. Jacobsen, *Adv. Synth. Catal.* **2002**, *344*, 953–956.

Received: November 28, 2006
Published online: March 13, 2007

